

Growth, overprinting, and stabilization of Proterozoic Provinces in the southern Lake Superior region

Daniel Holm^{a,*}, L. Gordon Medaris, Jr.^b, Kalin T. McDannell^c, David A. Schneider^d, Klaus Schulz^e, Bradley S. Singer^b, Brian R. Jicha^b

^a*Dept. of Geology, Kent State University, Kent, OH*

^b*Dept. of Geoscience, UW-Madison, WI*

^c*Geological Survey of Canada, Calgary, AB*

^d*Dept. of Earth Science, University of Ottawa, Ottawa, ON*

^e*U.S. Geological Survey, Reston, VA*

Abstract

New geochronologic data in the southern Lake Superior region provide key information on the timing and nature of tectonic activity that pre-and post-date initial Paleoproterozoic growth of Laurentia during the geon 18 Penokean orogeny. The obducted Pembine ophiolite formed along the edge of a Paleoproterozoic ocean basin at least 30 m.y. prior to Penokean island arc/microcontinent accretion beginning at 1860 Ma. Following Penokean orogenesis, intrusion of mafic dikes at 1817 ± 2 Ma indicate a period of extension that coincided with a 30 m.y. gap in orogenic felsic magmatism at 1835-1805 Ma (between the Penokean and Yavapai orogenies) and likely represents relaxation of Penokean compression and a tectonic switch to intra-arc extension related to initiation of Yavapai subduction. Subsequent Yavapai arc accretion (1750-1720 Ma) resulted in pervasive ductile deformation of the dikes and host rocks at temperatures of ~ 700 °C, previously attributed to Penokean deformation. Geon 16 Mazatzal overprinting of the accreted Penokean and Yavapai provinces was widespread but of overall lower metamorphic grade (greenschist facies), and the thermal effects of the 1476-1470 Ma shallow level Wolf River batholith was limited to a 10-15 km wide contact zone surrounding the intrusion.

In contrast to the Archean Superior Province to the north, Paleoproterozoic terranes in the southern Lake Superior area experienced widespread low-temperature reheating and cooling of shallow crustal levels at ca. 1.1-1.0 Ga attributed primarily to magmatic underplating with little subsequent Neoproterozoic exhumation. In the southern Lake Superior region widespread magmatic underplating likely thickened, strengthened, and stabilized Proterozoic Penokean-Mazatzal lithosphere but destabilized Archean cratonized Superior Province lithosphere to the north.

* Corresponding author: Dept of Geology, 325 S. Lincoln Street, Kent State University, Kent, OH 44242, USA. dholm@kent.edu.

Keywords: geochronology, mafic magmatism, Proterozoic tectonics, stabilization, Penokean, Yavapai, thermochronology

1. Introduction

Proterozoic continental growth following assembly of the Laurentian core is conventionally attributed to successive accretion of numerous juvenile arcs along the margins of the Archean Superior and Wyoming provinces (Karlstrom et al., 2001). Late Paleoproterozoic (1900-1600 Ma) juvenile arc rocks in the upper Great Lakes region formed during three separate accretionary tectonic episodes as the North American craton grew southward (Fig. 1; NICE Working Group, 2007).

The oldest of these accretionary orogens, the 1875-1835 Ma Penokean province (Van Schmus, 1980), is located in the southern Lake Superior region (Wisconsin, northern Michigan, east-central Minnesota, and southwestern Ontario). The Penokean province includes many of the

hallmarks of accretion, including an ophiolite-island arc complex, the Pembine ophiolite, that was obducted along the Niagara fault, a Paleoproterozoic suture zone (Schulz and Cannon, 2007)

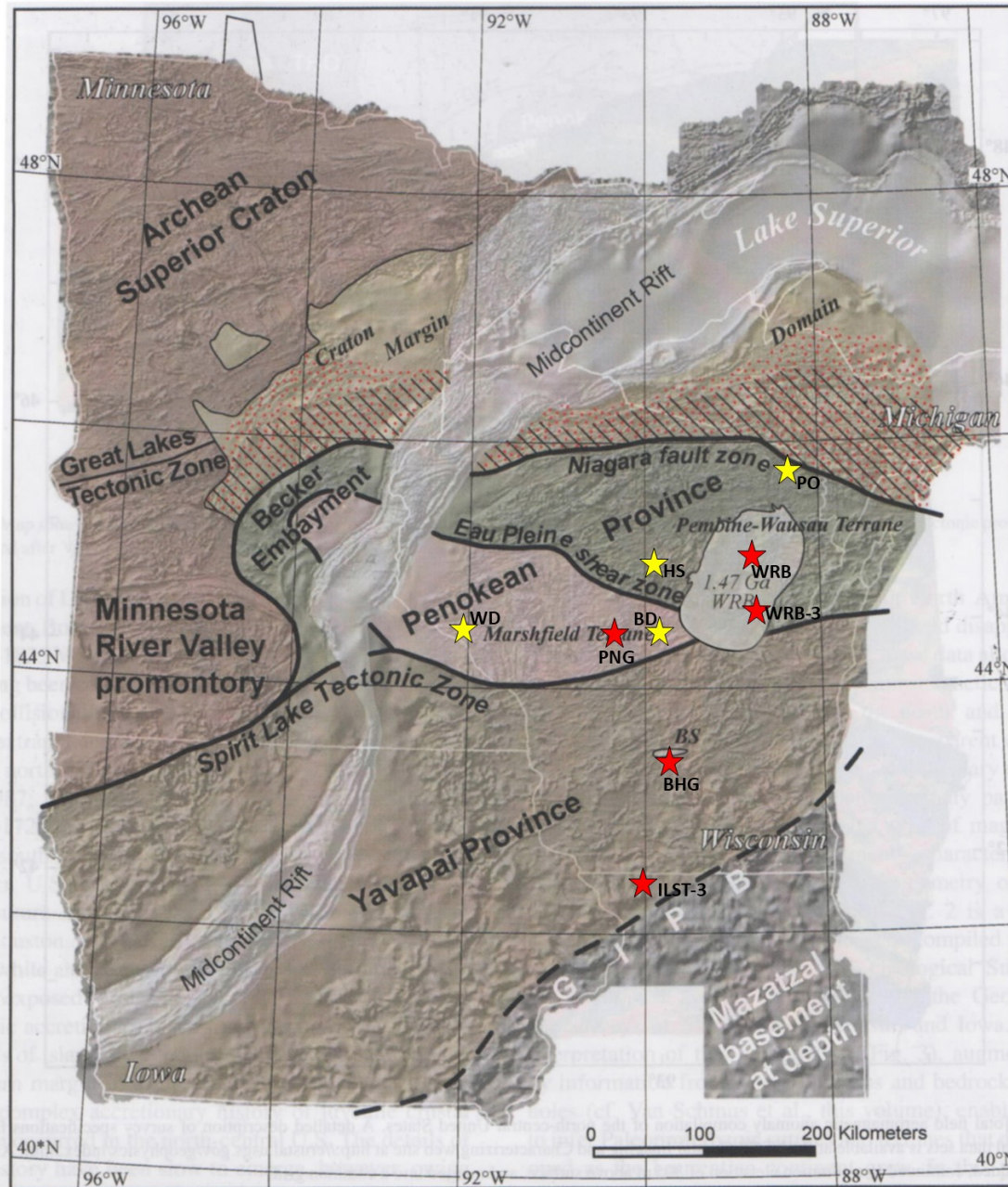


Fig. 1: Geologic terrane map of Precambrian basement rocks in the northern U.S. continental interior (after NICE Working Group, 2007). Yellow stars represent localities with higher temperature age data discussed in the text (BD: Biron dam; HS: Hamburg schist; PO; Pembine ophiolite; WD: Wissota dam). Red stars represent localities with low-T feldspar Ar/Ar ages (PNG: geon 18 Neillville granite; BHG: geon 17 Baxter Hollow granite; ILST-3: geon 14 granite core; WRB and WRB-3: geon 14 Wolf River granite).

The Penokean terrane was variably overprinted by magmatic, tectonic, and thermal episodes associated with pulses of geon 17 (Yavapai), geon 16 (Mazatzal), geon 14 (Wolf River batholith) and geon 11 (Mid-Continent Rift) tectonomagmatic events. Determining the timing, nature and relative contribution of these subsequent events is critical for properly ascribing structures, strain features, and degree of metamorphism/reheating to their correct tectonomagmatic event (Craddock et al., 2018). In this paper, we present geochronologic data that provide key information on the timing, extent, and nature of tectonic activity that bounds and overprints the Penokean orogeny.

The Pembine ophiolite formed at least 30 m.y. prior to initial accretion of the Penokean island arc with the southern margin of the Superior craton at 1860 Ma. Following Penokean orogenesis, a temporary switch to tectonic extension occurred at 1817 Ma during a 30 m.y. hiatus between the end of Penokean magmatism at 1835 Ma and the start of Yavapai magmatism at 1805 Ma. Additionally, geothermometry and thermochronologic data enable us to document strong penetrative geon 17 (Yavapai) ductile deformation and metamorphism of the southern Penokean orogen north of the Spirit Lake tectonic zone and more limited metamorphic overprinting associated with geon 16 Mazatzal accretion and subsequent emplacement of the geon 14 Wolf River batholith. Finally, low temperature geon 11-10 cooling occurred subsequent to widespread reheating related to geon 11 mantle plume heating and magmatic underplating that ultimately strengthened and stabilized the amalgamated Proterozoic continental lithosphere, while destabilizing Archean lithosphere to the north.

2. Tectonic setting of the southern Lake Superior region

In the southern Lake Superior region, the 1875-1835 Ma Penokean orogeny represents an island-arc/microcontinent collision that deformed and metamorphosed Archean basement and ca. 2100 Ma continental passive margin rocks (Schulz and Cannon, 2007; Fig. 1), some of which may be as young as ca. 1900 Ma (Pietrzak-Renaud and Davis, 2014). In northern Wisconsin, the steep, south-dipping Niagara fault zone (NFZ) is interpreted to be an 1860 Ma suture that separates deformed continental margin rocks on the north from tholeiitic and calc-alkalic volcanic and plutonic arc rocks of the Wisconsin magmatic terranes (WMT) to the south. The WMT consists of a northern primitive oceanic to evolved island arc-complex, the Pembine-Wausau terrane, that is separated from a southern exotic Archean microcontinent, the Marshfield terrane, by the steeply south-dipping Eau Pleine shear zone (EPSZ), also interpreted as a paleo-suture. Penokean volcanic and plutonic rocks (Sims et al., 1989; Van Wyck, 1995), which overlie and intruded the Archean gneisses of the Marshfield terrane, are deformed into steeply plunging folds with associated steep stretching lineations. The strong ductile deformation and coeval metamorphism of the Penokean igneous rocks has been historically attributed solely to Penokean orogenic deformation (Myers et al., 1980; Maass et al., 1980; Maass, 1983). Undeformed granites emplaced between 1836 and 1834 Ma (Sims et al., 1989; Schneider et al., 2002) pierce the Niagara and the Eau Pleine sutures and mark the upper bound on the timing of Penokean orogenesis (Schulz and Cannon, 2007).

Following a 30 m.y. hiatus in magmatism after Penokean orogenesis, renewed felsic plutonism beginning at 1805 Ma (Humboldt granite, northern MI) heralded the onset of abundant long-lived (50 m.y.) magmatism that generally migrated southeastward across the accreted Penokean crust and may be related to a slab window or slab breakoff event associated with northwest-directed subduction of Yavapai oceanic lithosphere beneath the newly accreted

Penokean terrane (Holm et al., 2005). In central Wisconsin (Fig. 1), aeromagnetic data indicate that the Penokean Marshfield and Pembine-Wausau terranes and the Eau Pleine shear zone are truncated by the east-northeast trending Spirit Lake tectonic zone (SLTZ), interpreted to be a northerly dipping Yavapai-age suture (NICE Working Group, 2007; Chichester et al., 2018). Yavapai arc accretion along the SLTZ likely occurred between 1750 and 1700 Ma, prior to deposition of Baraboo Interval supermature quartzites, which blanketed both the Penokean and Yavapai terranes (Dott, 1983; Holm et al., 1998b; Medaris et al., 2003; Schwartz et al., 2018; Stewart et al., 2018).

Archean gneisses and Paleoproterozoic continental margin rocks north and west of the NFZ underwent two episodes of medium pressure amphibolite-facies metamorphism; first during tectonic burial associated with Penokean accretion and second, associated with Yavapai magmatism (primarily east-central Minnesota, Holm et al., 1998a) and coeval gneiss dome formation during collapse and exhumation of the overthickened Penokean orogenic crust (primarily northern Michigan; Schneider et al., 2004). South of the NFZ throughout the Pembine-Wausau terrane in Wisconsin, metamorphism varies from upper greenschist to middle amphibolite facies (Geiger and Guidotti, 1989).

The geon 17 Yavapai tectonomagmatic event was followed by late geon 16 Mazatzal terrane accretion (Karlstrom and Bowring, 1993; Karlstrom et al., 2001), which (re)metamorphosed much of the previously accreted Penokean and Yavapai arc terranes (Dott, 1983; Holm et al., 1998b, 2007). In northwestern Wisconsin, Holm et al. (1998b) inferred the existence of a Mazatzal-age tectonic front, marked by the northern limit of folded quartzite spatially coinciding with reset (<1620 Ma) $^{40}\text{Ar}/^{39}\text{Ar}$ mica ages in basement rocks, which interestingly, also roughly coincides with the trace of the NFZ. Mazatzal-age metamorphism in much of Wisconsin is largely greenschist facies, having reached regional amphibolite facies only further

south in crust more proximal to the Mazatzal/Yavapai tectonic boundary (NICE Working Group, 2007; Van Schmus et al., 2007). New detrital zircon ages from the folded Waterloo quartzite and Baldwin conglomerate in Wisconsin establish post-Mazatzal deposition for some of the Proterozoic quartzites, and $^{40}\text{Ar}/^{39}\text{Ar}$ ages for axial-planar muscovite in the Seeley Slate, Baraboo Quartzite, and Waterloo Quartzite indicate subsequent deformation during the ca. 1470–1460 Ma Wolf River tectonomagmatic event (Medaris et al., 2018, 2019; Schwartz et al., 2018).

South of the SLTZ, the geophysical character of the crust throughout southern Wisconsin indicates that much of the Mazatzal and Yavapai arc terranes were intruded by the ca. 1475–1430 Ma granites of the Eastern Granite Rhyolite Province, part of an extensive suite of magmatism that transects much of the southern part of the North American continent (Anderson, 1983). One of the oldest and largest intrusive bodies of this suite, the 1470–1476 Ma Wolf River batholith (Dewane and Van Schmus, 2007) and associated plutons in central Wisconsin, intruded juvenile rocks of the Penokean province mostly north of the Spirit Lake tectonic zone (Fig. 1). $^{40}\text{Ar}/^{39}\text{Ar}$ plateau ages of 1450–1470 Ma from fine-grained muscovite in Baraboo Interval quartzites reflect widespread, but stratigraphically localized, hydrothermal activity and potassic metasomatism related to the Wolf River tectonomagmatic event (Medaris et al., 2003). $^{40}\text{Ar}/^{39}\text{Ar}$ biotite cooling ages from the WRB are only slightly younger than its intrusive age (ranging from 1460 to 1415 Ma) consistent with shallow emplacement (Holm and Lux, 1998; Holm et al., 2007).

The final Proterozoic crust-forming event in the southern Lake Superior region was aborted intracontinental rifting at 1100 Ma that created the Midcontinent Rift System (MRS; Van Schmus and Hinze, 1985; Hinze et al., 1997). MRS magmatism produced a profound magnetic and gravity anomaly that can be traced for 2500 kilometers along an arcuate path across the midcontinent (Fig. 1), with its location in the Lake Superior region influenced by the shape of the Paleoproterozoic (2.3–1.9 Ga) pre-Penokean craton margin (Ola et al., 2016).

3. Pre and post-Penokean mafic magmatism

3.1 Pembine ophiolite in northeast Wisconsin

The dismembered Pembine suprasubduction zone ophiolite (Schulz, 1987) is located within the Pembine-Wausau terrane south of the Niagara suture zone in northeastern Wisconsin (locality PO, Fig. 1). As described in LaBerge et al. (2003), the ophiolite is composed of mid-ocean ridge-type basalts and gabbros, primitive island-arc tholeiitic pillow basalt and diabase, boninitic pillowed flows and breccias, and massive to layered peridotite-gabbro bodies locally intruded by sheeted mafic dikes, and ultramafic rocks (pyroxenites and serpentinites). The ophiolite sequence is overlain to the south by low-K calc-alkaline andesite to rhyolite lava flows and volcanoclastic rocks with oceanic-arc compositional characteristics and is intruded by syn-volcanic diorite-quartz diorite-tonalite bodies as well as syn- to post-tectonic diorite-tonalite-granite plutons. One of these, the Twelve Foot Falls quartz diorite, is a large 20 km x 5 km sill-like pluton, which intrudes the upper part of the ophiolite sequence and is in fault contact with calc-alkaline volcanic rocks (Fig. 2; Sims and Schulz, 1993). The quartz diorite is similar in chemical composition to low-K primitive calc-alkaline andesites (Sims et al., 1992).

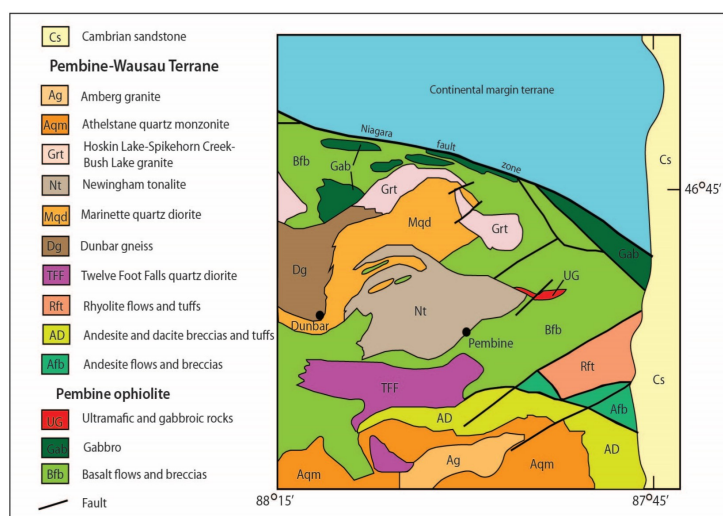


Fig. 2: Simplified geology of the Pembine-Wausau terrane in northeast Wisconsin showing the Pembine ophiolite and Twelve Foot Falls quartz diorite (after Sims and Schulz, 1993).

3.2 Mafic dikes of central Wisconsin

Strongly deformed Precambrian rocks exposed along and near the Wisconsin River in central Wisconsin (between Stevens Point and Wisconsin Rapids) occur at the nexus of where the 1475 Ma Wolf River batholith intrudes the Penokean WMT and the Yavapai SLTZ (locality BD, Fig. 1). Precambrian basement in this area consists of Archean tonalitic to dioritic gneiss and migmatite and a variety of Penokean igneous rocks, including tonalite, granodiorite, and granite (Sims et al., 1989; Van Wyck, 1995). Many of the igneous rocks have been re-crystallized, exhibiting a range of planar and linear fabrics. Subvertical east-northeast striking diabase dikes, now recrystallized to amphibolite, intrude the deformed Penokean igneous rocks (Fig. 3; Maass et al., 1980).

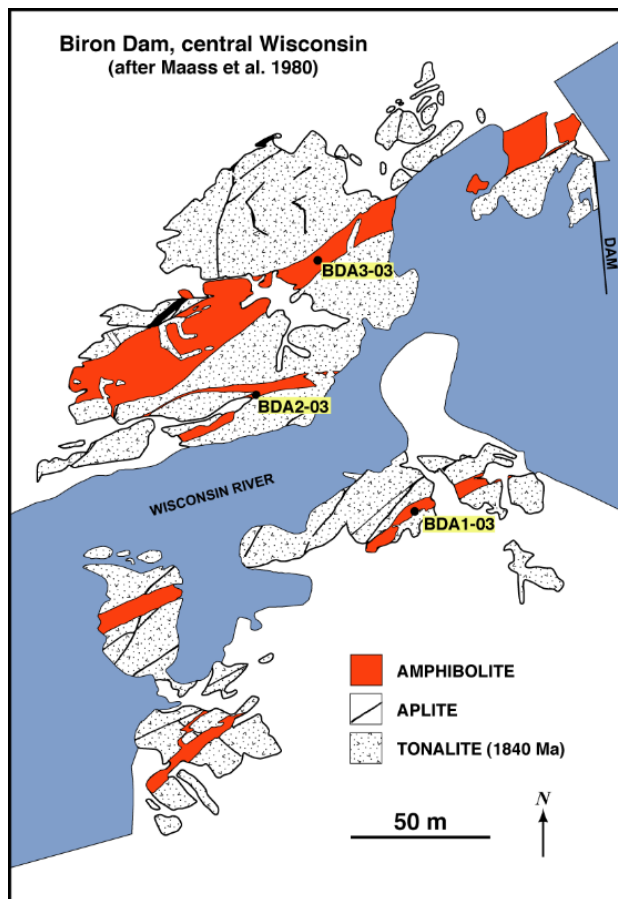


Fig. 3: Geologic map of the Biron dam area, showing the distribution of Penokean tonalite, aplite dikes and metadiabase dikes with sample localities.

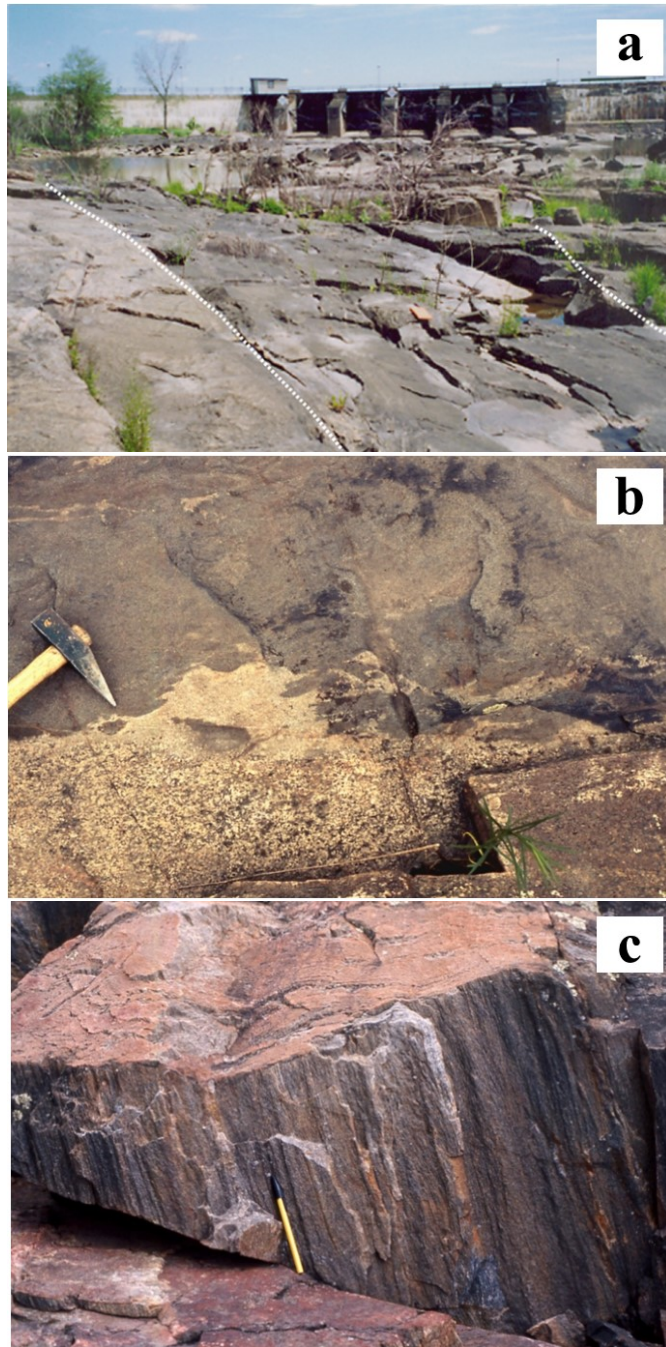


Fig. 4: a) Photo of Biron dam with sharp dike contacts (dotted lines) and tonalite in the foreground. b) Photo of Biron dam dike contact showing partial melting and rheomorphic veining. c) Photo of strongly lineated tonalite at Conants Rapids.

The dike margins have not been severely deformed and maintain sharp cross-cutting contacts with the ca. 1840 Ma Penokean tonalites they intruded (Fig. 4a; Van Wyck, 1995), including local preservation of melting in tonalite at contacts with the metadiabase (Fig. 4b).

The metadiabase dikes are trachybasalt in composition, containing 50.6–51.4 wt% SiO₂ and 5.0–5.3 wt% Na₂O+K₂O, and having Mg-numbers (100 x molar MgO/[MgO+FeO]) of 48.6–55.0. Samples collected from three of the dikes are close to silica saturation, with BDA–1 containing 0.46 wt.% normative quartz and BDA–2 and BDA–3 containing 1.15 and 1.20 wt% normative olivine, respectively. In terms of trace elements, the trachybasalt exhibits a pronounced subduction signature that is characterized by negative anomalies for Nb and Ta, Sr, P, Zr and Hf, and Ti, and a strongly positive anomaly for Pb (Fig. 5). With relatively high K₂O, Th and light REE contents, the trachybasalt most resembles calc-alkaline continental arc basalt (Murphy, 2007).

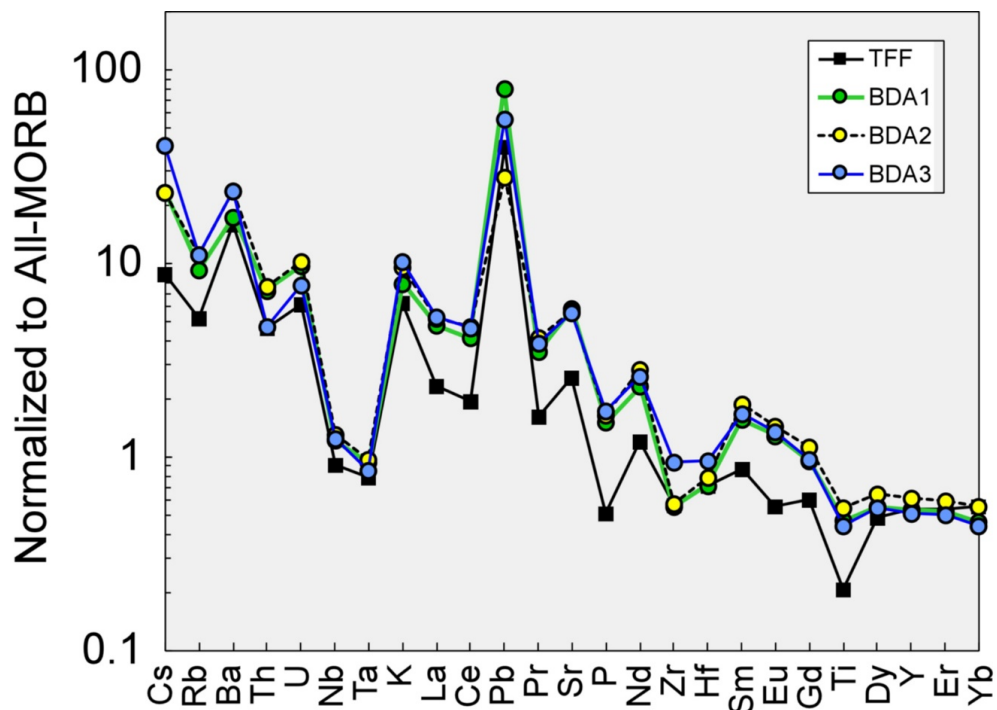


Fig. 5: Extended trace element plot of Twelve Foot Falls quartz diorite and metadiabase dikes at Biron dam, normalized to All-MORB (Gale et al., 2013).

Except for a few unmetamorphosed ca. 1100 Ma MRS diabase dikes, all rock units have been metamorphosed under amphibolite-facies conditions and possess a steeply plunging, penetrative mineral lineation (Fig. 4c). Detailed mapping and structural analysis document three steeply plunging sets of isoclinal to open folds with fold axes that parallel the prominent mineral lineation (Maass et al., 1980). Holm et al. (2007) reported an $^{40}\text{Ar}/^{39}\text{Ar}$ plateau age of 1600 ± 5 Ma on biotite separated from one of the amphibolite dikes indicating the dikes must be late Paleoproterozoic in age (between 1840 and 1600 Ma).

4. Analytical methods

4.1 U-Pb geochronology

Zircon was separated from 2 kg rock samples using standard mineral separation techniques. The handpicked zircon grains were mounted in epoxy and polished and imaged using a scanning electron microscope. All isotopic measurements were made using the CAMECA ims1270 ion microprobe housed within the National Ion Microprobe Facility at the University of California, Los Angeles. The U-Pb measurements were made with a $\sim 20 \mu\text{m}$ O^- beam according to the methods of Schmitt et al. (2003) for analyses of polished zircon. Zircon standard AS3 (1099 ± 1 Ma; Paces and Miller, 1993) was used to determine the relative sensitivities for Pb and U of the unknowns using a calibration technique similar to Compston et al. (1984). U-Pb isotopic ratios and ages were calculated from measured ion intensities, using in-house software written by C.D. Coath (ZIPS v3.4), and are corrected for ^{204}Pb . Isoplot v3.0 (Ludwig, 2003) was used to plot weighted mean, age probability diagrams and Concordia diagrams. Results are presented in Supplementary Table 1 and Figure 6. Errors on individual spot ages are reported at the 1σ level and weighted mean ages are presented at the 95% level of confidence (2σ level) based on the $^{207}\text{Pb}/^{206}\text{Pb}$ isotopic ratios.

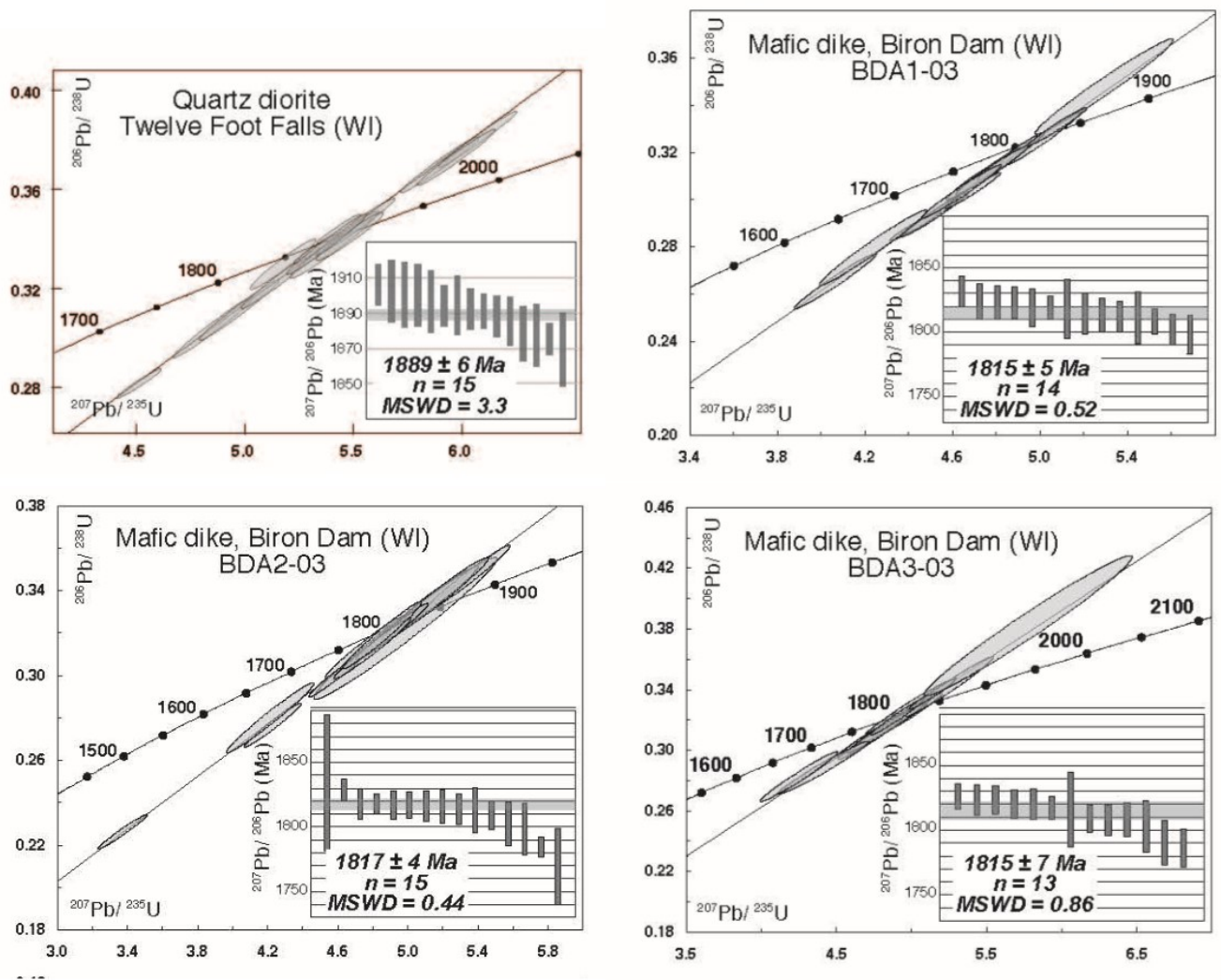


Fig. 6: Zircon U-Pb Concordia plots from Twelve Foot Falls quartz diorite (1889 Ma) and three metadiabase dikes at Biron dam (all 1817 Ma).

4.2 $^{40}\text{Ar}/^{39}\text{Ar}$ thermochronology

$^{40}\text{Ar}/^{39}\text{Ar}$ incremental analyses using a defocused CO_2 laser beam were performed at the University of Wisconsin Rare Gas Geochronology Laboratory with procedures like those of Smith et al. (2006). Several samples of amphibolite containing medium-grained hornblende, one sample of schist containing muscovite, and two samples of microcline-bearing granite were crushed to 250-500 μm . A few milligrams of hornblende, muscovite, and microcline grains were handpicked and then irradiated in the CLICIT facility (cadmium-shielded) of the Oregon State

University nuclear reactor for 40 h. The conversion efficiency of ^{39}K - ^{39}Ar was monitored using sanidine from the 28.34 Ma Taylor Creek Rhyolite (Renne et al., 1998). Based on the monitors, the neutron fluence parameter J is 0.010402 ± 0.000052 (2σ). Corrections for interfering nuclear reactions are based upon previous measurements on synthetic K-glass and CaF_2 salts (Supplementary Table 2). A five-grain aliquot of sample was placed in a well on a copper disc and heated 2 min for each gas increment released, with laser output power varying from 1 to 6 W. The released gas was purified for 5 min with two SAES GP-50 getters and admitted into a MAP 215-50 mass spectro-meter for Ar isotope analysis using an electron multiplier. System blanks were measured before and after every three analyses, and data were corrected for blanks and mass-fractionation effects. Final data reduction was via ArArCalc (Koppers, 2002). Results are given in Supplementary Table 2 and Figure 7. The uncertainty in age reflects analytical uncertainties only at the 2σ level.

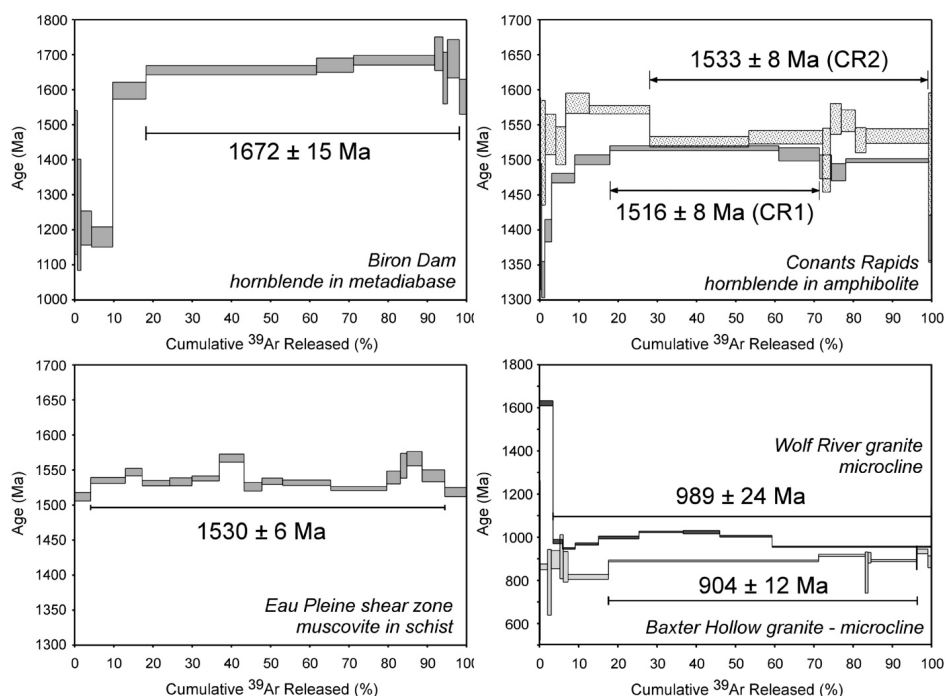


Fig. 7: $^{40}\text{Ar}/^{39}\text{Ar}$ degassing spectra from central Wisconsin. a) hornblende from metadiabase dike; Biron dam; b) hornblende from amphibolite lenses in Archean gneiss at Conants Rapids <10 km from Wolf River batholith; and c) muscovite from the Eau Pleine shear zone. d) microcline from the 1476 Ma Wolf River granite and 1750 Ma Baxter Hollow granite.

Nominal closure temperatures of 500 °C for hornblende, 350 °C for muscovite, and below 300 °C but above 150 °C for potassium feldspar are used (cf. McDougall and Harrison, 1999).

4.3 $^{40}\text{Ar}/^{39}\text{Ar}$ K-feldspar multi-diffusion domain (MDD) thermochronology

$^{40}\text{Ar}/^{39}\text{Ar}$ analysis of K-feldspar using the MDD method has been utilized in a number of laboratory experiments (Harrison et al., 1991; Lovera et al., 1989, 1993, 1997, 2002) and has recently been successfully applied to link higher and low-temperature thermochronological systems from well-constrained cratonic localities (McDannell et al., 2018). $^{40}\text{Ar}/^{39}\text{Ar}$ K-feldspar MDD analysis is able to determine continuous temperature-time paths over the range ~150 to ~300 °C. $^{40}\text{Ar}/^{39}\text{Ar}$ step-heating analyses were performed on potassium feldspar at the Lehigh University noble gas laboratory using the methodology described in McDannell (2017) and McDannell et al. (2018).

Additional samples of granites (described below) were crushed, sieved to 250 μm , and separated using methylene iodide to isolate the feldspar fraction. Approximately 1.0-1.5 mg of feldspar per sample was handpicked and irradiated with K and Ca salts and GA1550 biotite flux monitors at the Oregon State University CLICIT nuclear reactor for 50 h. Samples were outgassed using incremental (isothermal duplicate) step heating by a double-vacuum resistance furnace with a Mo crucible over 54 heating steps from 450-1450 °C, with multiple isothermal steps at 1100 °C to extract as much gas as possible before sample melting. The automated extraction system fitted with SAES GP-50 getters is connected to a Thermo Argus VI multi-collector mass spectrometer operated at 4.5 kV accelerating potential and 200 mA trap current. Under these conditions, the background for ^{36}Ar is 1×10^{-14} cc STP. Routine Ar analyses are performed in multi-collector mode using Faraday detectors to measure ^{40}Ar , ^{39}Ar , ^{38}Ar and ^{37}Ar ,

and either a fifth Faraday detector or an ion-counting electron multiplier is used to measure ^{36}Ar . Furnace temperature is monitored by a W-Re thermocouple and a laser extraction line is outfitted with a Merchantek CO_2 laser operated with a continuous 10.6 μm beam (variable output power up to 35 W) for fusion of Ca and K salts for calculating the mass discrimination factor and mass interferences. The GA-1550 biotite standard (98.5 ± 0.5 Ma; McDougall and Wellman, 2011) is also outgassed for neutron flux monitoring to determine irradiation constants.

Raw mass spectrometer data are reduced using ArArCalc (Koppers, 2002) and beam values are regressed to the time of gas inlet and corrected for background, line blank, discrimination, decay of ^{37}Ar and ^{39}Ar , and Ca and K-derived nucleogenic interferences. All $^{40}\text{Ar}/^{39}\text{Ar}$ step ages are accompanied by propagation of uncertainties due to line blank, mass discrimination, peak-height regressions, nucleogenic interferences, flux monitor measurements, J-factor interpolation, and decay constants. All raw $^{40}\text{Ar}/^{39}\text{Ar}$ data discussed below are available from the online repository: <https://preserve.lehigh.edu/etd/2721>.

4.4 Inverse thermal modeling of MDD data

Data derived from MDD thermochronology (i.e., the sample's specific diffusion kinetics and domain-size distribution) can be used to invert the MDD age spectrum to its thermal history. Inverse thermal history modeling of MDD data was carried out following the methods outlined in McDannell et al. (2018), by first using the *domains* program to invert the laboratory-derived kinetic data and heating schedule for feldspar domain structure. The same approach was taken for each sample when modeling the diffusion domain distribution: (1) use of a slab diffusion geometry; (2) modeling was only performed up to 1050-1100 $^{\circ}\text{C}$, just before typical K-feldspar melting temperature; (3) the number of diffusion domains were allowed to be between 3 and 10; and (4) The E_a and $\log D_0/r^2$ values must all be within the range reported in the large database of

>100 samples by Lovera et al. (1997). After data reduction, samples were only considered for inverse modeling if there was acceptable cross-correlation (Lovera et al., 2002) between the observed age spectrum and the $\log R/R_0$ spectrum determined from ^{39}Ar release kinetics: a good correlation (>0.9) supports the fundamental requirement that ^{40}Ar and ^{39}Ar diffusion are occurring in the same manner. Inversion of the diffusion domain information for thermal history was carried out using the *Arvert* v. 5.11 software (Zeitler, 2004; Harrison et al., 2005) employing random Monte Carlo exploration with the enhanced learning component of the controlled random search (CRS) algorithm (Price, 1977; Willett, 1997). The only imposed *Arvert* model constraints were that maximum heating and cooling rates were required to be $\leq 2\text{-}3^\circ\text{C}/\text{My}$ and only MDD data were modeled during simulations. The Wolf River batholith sample was also modeled using QTQt v. 5.7 (Gallagher, 2012) utilizing the Bayesian Markov-chain Monte Carlo method for comparison to the CRS results. The QTQt model was a total of 550,000 iterations with the only imposed constraints being maximum allowed rates of $dT/dt = 2^\circ\text{C}/\text{My}$, the published biotite $^{40}\text{Ar}/^{39}\text{Ar}$ data of Holm and Lux (1998) as a high-temperature constraint, and a Cambrian ($25 \pm 15^\circ\text{C}$ at $520 \pm 20\text{ Ma}$) near-surface constraint, in agreement with the regional preserved stratigraphy.

4.5 Electron microprobe geothermometry

Minerals were analyzed by wavelength-dispersion spectrometry (WDS) with a Cameca SX50 instrument at the University of Wisconsin-Madison. Operating conditions were 15 kV accelerating voltage, 20 nA beam current (Faraday cup) for amphibole and 10 nA for plagioclase, and beam diameter of 1 μm for amphibole and 5 μm for plagioclase. Combinations of natural minerals were used as standards, e.g. amphibole for Si, Al, Fe, Mg, and Ca, rutile for Ti, rhodonite for Mn, jadeite for Na, and microcline for K in unknown amphibole, and natural

oligoclase and andesine for unknown plagioclase. Data reduction was performed by Probe for Windows software, utilizing the $\phi(\rho z)$ matrix correction of Armstrong (1988). Major element abundances are estimated to be precise within $\pm 3\%$, and minor element abundances, within $\pm 10\%$, based on replicate analyses. The proportion of ferric iron in amphibole was estimated from charge balance considerations, following the method of Schumacher (1997). Representative amphibole and plagioclase compositions in Biron dam and Conants Rapids metadiabases are given in Table 3.

Table 3. Representative amphibole and plagioclase compositions from 1817 Ma metadiabase dikes

Mineral	Amphibole			Plagioclase			
	Locality	Locality		Locality	Locality		
	<u>Biron Dam</u>	<u>Conants Rapids</u>		<u>Biron Dam</u>	<u>Conants Rapids</u>		
Sample	86GM100	01CR1A	01CR2A	Sample	86GM100	01CR1A	01CR2A
# of analyses	29	25	25	# of analyses	45	45	45
wt. %	wt. %			wt. %			
SiO ₂	42.74	41.68	42.88	SiO ₂	58.10	62.51	62.57
TiO ₂	0.65	0.67	0.58	Al ₂ O ₃	26.69	23.27	23.94
Al ₂ O ₃	11.40	10.06	9.48	Fe ₂ O ₃	0.08	0.09	0.10
FeO _{Total}	16.07	20.47	19.13	CaO	8.31	4.65	5.15
MnO	0.29	0.33	0.36	Na ₂ O	6.61	8.59	8.21
MgO	10.57	8.38	9.42	K ₂ O	0.07	0.20	0.19
CaO	11.67	11.58	11.71	Sum	99.87	99.32	100.15
Na ₂ O	1.25	1.25	1.16				
K ₂ O	0.62	1.13	1.01	<i>cations per 5 oxygen atoms</i>			
Sum	95.27	95.56	95.73	Si	2.599	2.783	2.763
<i>cations after Schumacher (1997)</i>				Al	1.407	1.221	1.246
<i>T-site</i>				Fe ³⁺	0.003	0.003	0.003
Si	6.476	6.473	6.588	Ca	0.398	0.222	0.244
Al IV	1.524	1.527	1.412	Na	0.573	0.742	0.703
Sum	8.0	8.0	8.0	K	0.004	0.011	0.010
<i>C-site</i>				Σ Cations	4.985	4.982	4.969
Al VI	0.513	0.314	0.305	<i>% end members</i>			
Cr	0.000	0.000	0.000	An	40.8	22.8	25.5
Fe ³⁺	0.488	0.536	0.507	Ab	58.8	76.0	73.4
Ti	0.075	0.078	0.068	Or	0.4	1.2	1.1
Mg	2.388	1.941	2.157				
Fe ²⁺	1.548	2.122	1.951				
Mn	0.038	0.043	0.047				
Sum	5.0	5.0	5.0				
<i>B-site</i>							
Ca	1.895	1.927	1.927				
Na	0.056	0.039	0.039				
Sum	2.0	2.0	2.0				
<i>A-site</i>							
Na	0.253	0.336	0.307				
K	0.119	0.225	0.198				
Sum	0.372	0.561	0.505				
Σ Cations	15.373	15.561	15.506				

5. Results

5.1 U-Pb geochronology

5.1.1 Twelve Foot Falls Quartz Diorite, Pembine, Wisconsin

Previous attempts to date the volcanic components of the Pembine ophiolite were unsuccessful because of a lack of recoverable zircon, probably caused by the generally low zirconium content of these primitive arc rocks. However, we were able to separate magmatic zircons from the Twelve Foot Falls quartz diorite, a gray, generally medium- to coarse-grained quartz diorite containing crystals of subhedral sodic andesine, subhedral hornblende, and anhedral bluish quartz (Sims et al., 1992).

Zircon grains are colorless and mostly doubly terminated euhedral grains. A total of 15 spots on nine zircon grains were analyzed. The Th/U values are generally <0.5 . The ages range from 1875 to 1905 Ma that define a discord with a weighted mean $^{207}\text{Pb}/^{206}\text{Pb}$ age of 1889 ± 6 Ma (MSWD: =3.3; Fig. 6a and Supplementary Table 1).

5.1.1 Metadiabase dikes, central Wisconsin

Three amphibolitized mafic dikes were sampled along the Wisconsin River below Biron dam, ~ 6 kilometers north of Wisconsin Rapids (Fig. 3). The dikes are black and fine- to medium-grained and interpreted to be metamorphosed diabase intrusions (Maass et al., 1980). The mineralogy of the dikes consists of plagioclase (An_{41}) + amphibole (magnesiohornblende) + titanite + apatite \pm biotite \pm epidote \pm quartz. Steeply aligned amphibole grains define a strong nematoblastic fabric.

Separated zircon grains are pink and mostly subhedral with slight overgrowths. The results for the three samples are plotted on Concordia diagrams (Fig. 6 b, c, d) and the isotopic

analyses are given in Supplementary Table 1. Age data are reported as $^{207}\text{Pb}/^{206}\text{Pb}$ ages and were used to calculate weighted averages. Like the quartz diorite that was dated, the Th/U values are quite low.

A total of 14 spots on twelve zircon grains from sample BDA1-03 were analyzed. The ages range from ca. 1830 to 1800 Ma with a weighted mean $^{207}\text{Pb}/^{206}\text{Pb}$ age of 1815 ± 5 Ma (MSWD: 0.52) for all spots. A total of 15 spots on 14 zircon grains from BDA2-03 were analyzed, with ages ranging from about 1830 to 1770 Ma with a weighted mean $^{207}\text{Pb}/^{206}\text{Pb}$ age of 1817 ± 4 Ma (MSWD: 0.44) for all 15 spots.

A total of 13 spots on ten zircon grains from BDA3-03 were analyzed yielding ages from ca. 1830 to 1790 Ma and resulting in a weighted mean $^{207}\text{Pb}/^{206}\text{Pb}$ age of 1815 ± 7 Ma (MSWD: 0.86) for all 13 spots. The weighted mean ages for the three samples all fall within error of each other and when combined result in weighted mean $^{207}\text{Pb}/^{206}\text{Pb}$ age of 1817 ± 2 Ma with an MSWD of 0.70.

5.2 $^{40}\text{Ar}/^{39}\text{Ar}$ thermochronology

$^{40}\text{Ar}/^{39}\text{Ar}$ laser step-heating of hornblende from a metadiabase dike at Biron dam (the same locality from which we obtained U-Pb zircon ages) yields a plateau age of 1672 ± 15 Ma for over 80% of the gas released (Fig. 7a). Biotite from metadiabase at Biron dam previously yielded a plateau age of 1600 ± 5 Ma (Holm et al., 2007). At Conants Rapids, ~17 km northeast of Biron dam, amphibolite occurs as slightly folded metadiabase dikes cross-cutting Archean gneiss and 1842 Ma foliated and lineated tonalites (Maass et al., 1980; Sims et al., 1989). Laser step-heating of hornblende from two of these mafic dikes yields plateau ages of 1516 ± 8 Ma and 1533 ± 8 Ma (Fig. 7b). Muscovite in low-grade schist, which was collected from the Eau Pleine shear zone

35 km north of Biron dam, yields an $^{40}\text{Ar}/^{39}\text{Ar}$ plateau age of 1530 ± 6 Ma for >90% of the gas released (Fig. 7c). Lastly, microcline separates from the Wolf River granite (location WRB, Fig. 1) and from the Baxter Hollow granite (sample BHG located in the Baraboo Range, Fig. 1) yielded Ar/Ar plateau ages of 989 ± 25 Ma and 904 ± 12 Ma respectively (Fig. 7d).

5.3 $^{40}\text{Ar}/^{39}\text{Ar}$ MDD thermochronology

Potassium feldspar separates were obtained from three Proterozoic granites for $^{40}\text{Ar}/^{39}\text{Ar}$ MDD analysis: the Penokean Neillsville granite (location PNG; Sims 1993), the geon 14 Wolf River granite (location WRB-3), and a geon 14 granite core sample from deep borehole UPH-3 (Hoppe et al., 1983) from the Illinois basement just south of Wisconsin (location ILST-3). Samples PNG and ILST-3 show evidence of excess Ar during early ^{39}Ar release. Furnace heating of K-feldspar from Wolf River granite sample WRB-3 (biotite $^{40}\text{Ar}/^{39}\text{Ar}$ age of ca. 1392 Ma; Holm and Lux, 1998) yields step ages ranging from ca. 970-380 Ma and an age spectrum indicative of slow cooling. The age spectrum shows plausible evidence of large diffusion domain breakage from crushing or minor recrystallization but yields an excellent $\log R/R_0$ cross-correlation of 0.99 (Fig. 8a). However, this sample is characterized by a low activation energy of ~ 159 kJ/mol, which is within the range of E_a reported in Lovera et al. (1997) but is below the ‘typical’ K-feldspar E_a of ~ 170 -210 kJ/mol (Reiners et al., 2005).

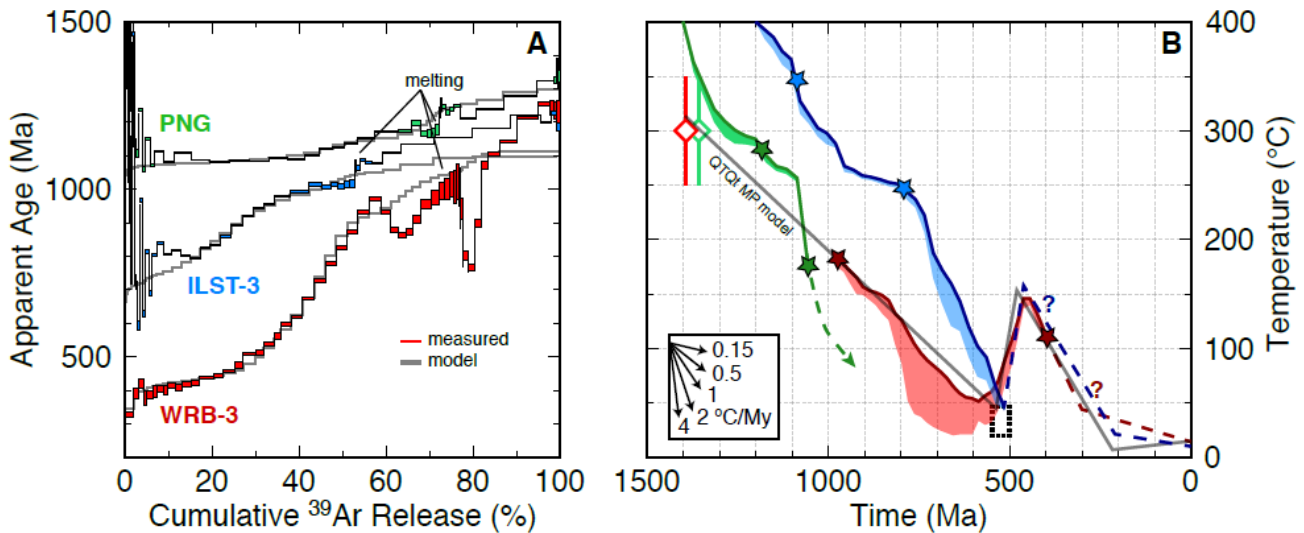


Fig. 8: $^{40}\text{Ar}/^{39}\text{Ar}$ age spectra and thermal history simulations for feldspar samples PNG, ILST-3, and WRB-3. (A) Age spectra showing apparent age vs. cumulative ^{39}Ar release. Measured age spectra (red) and Arvert model spectra (cyan). (B) Time-temperature plots showing Arvert model thermal history envelopes. Envelopes are T-t path bundle encompassing 150 T-t paths with the best-fitting path shown by heavy colored line. Gray line is the QTQt maximum posterior T-t history (Bayesian preferred model) for WRB-3 that is similar to the Arvert solution set. Dotted box is the Cambrian constraint used in the QTQt model. Modeled histories in panel B produce the model spectra in panel A. The stars denote the portion of the T-t path constrained by the Ar MDD data. Dashed lines are inferred T-t paths. Diamonds are published biotite $^{40}\text{Ar}/^{39}\text{Ar}$ data for PNG and WRB-3 with respective closure temperature range for the system.

Feldspar sample PNG (biotite $^{40}\text{Ar}/^{39}\text{Ar}$ plateau age of ca. 1357 Ma; Romano et al., 2000) exhibits apparent step ages ranging from ca. 1170 Ma to 1080 Ma and an age spectrum indicative of rapid cooling (Fig. 8a). The age spectrum for sample ILST-3 is characterized by step ages from ca. 1015-795 Ma. The late ^{39}Ar release (~45-52%) indicates relatively rapid cooling due to a plateau-like portion of the age spectrum that yields a weighted mean age of 1012.41 ± 1.46 Ma (2σ ; MSWD: 1.46, n: 6), followed by staircase-pattern step ages indicative of slow cooling (17-42% release) from 975 to 800 Ma.

Low temperature thermal history simulations of the MDD feldspar spectra suggest regionally variable lower temperature resetting and/or cooling of the Penokean and Yavapai

provinces in the Neoproterozoic. Time-temperature plots showing *Arvert* model thermal history envelopes for feldspar samples PNG, ILST-3, and WRB-3 are shown in Fig. 8b. The stars denote the portion of the T-t path constrained by the Ar MDD data. Inferred T-t paths depicted by dashed lines are discussed below.

5.4 Amphibole-Plagioclase geothermometry

Holland and Blundy (1994) have formulated geothermometers for two amphibole-plagioclase equilibria:

- 1) edenite + 4quartz = tremolite + albite, and
- 2) edenite + albite = richterite + anorthite.

Following these formulations, coexisting magnesiohornblende and andesine in metadiabase at Biron dam yield 725 °C and 658 °C for equilibria 1 and 2, respectively, at an assumed pressure of 6 kb (Table 4; the pressure dependence for equilibrium 1 is -1 °C/kb and for equilibrium 2 is +7 °C/kb). Of these two equilibria, the first is more appropriate, because metadiabase is close to being silica saturated, as previously described.

Two samples of amphibolite at Conants Rapids yield similar results for the same two equilibria, these being 713-725 °C and 628-632 °C, in this case for coexisting pargasite and oligoclase, again calculated for an assumed pressure of 6 kb. The pressure dependence in this case is -7 °C/kb for equation 1 and +4 °C/kb for equation 2.

Table 4. Temperature estimates for coexisting amphibole and plagioclase in Biron dam metadiabase and Conants Rapids amphibolite

Locality	Biron Dam	Conants Rapids	
Sample	86GM100	01CR1A	01CR2A
Equation A: edenite-tremolite			
P (kb) 2	729	751	739
6	725	725	713
10	722	698	686
Equation B: edenite-richterite			
P (kb) 2	630	617	612
6	658	632	628
10	686	648	643

6. Discussion

6.1 Minimum age of the Pembine ophiolite

The 1889 ± 6 Ma date for the Twelve Foot Falls quartz diorite sill provides a minimum age for the Pembine ophiolite and confirms that the ophiolitic sequence is older than most Paleoproterozoic rocks in the Pembine-Wausau magmatic terrane (mostly 1875-1835 Ma) and formed at least 30 m.y. before accretion of the Pembine-Wausau magmatic terrane to the southern margin of the Superior craton along the Niagara suture zone at ca. 1860 Ma. Several Paleoproterozoic mafic dike swarms, including the Marathon, Kapuskasing, Fort Frances, and recently identified dikes in northern Michigan (Schulz et al., 2018), are all ca. 2100 Ma and appear to mark the time of final rifting along the southern margin of the Superior craton (Halls et al., 2008; although Pietrzak-Renaud and Davis [2014] suggest at least local extension was occurring north of the Niagara Fault zone ca. 1890 Ma). Thus, there is approximately a 200 m.y. hiatus between rifting of the late Archean supercontinent Kenorland (Williams et al., 1991) and formation of the Pembine ophiolite before 1890 Ma and its obduction during Penokean island arc accretion along the Niagara fault zone. The new minimum age for the Pembine ophiolite suggests that a Paleoproterozoic ocean basin evolved following rifting of Kenorland at about

2200-2100 Ma, and that subduction systems in this ocean led to the generation of new arc crust and repeated accretion events along a Pacific-type southern margin of the Superior craton (Schulz and Cannon, 2007).

6.2 Origin of metadiabase dikes in the Penokean Province

The morphology of the zircon grains from the Biron dam metadiabase dikes and their low Th/U ratios suggest the zircons are magmatic in origin (Parrish, 1990). In addition, the 650-700 °C peak metamorphic conditions reached by these mafic rocks are below those required to produce new growth of zircon, and the basement arc rocks into which they intrude are 1840 Ma or older (Maass et al., 1980). Thus, we interpret the new ca. 1817 Ma U-Pb dates of these dikes to document an episode of mafic magmatism shortly after the end of Penokean orogenic magmatism (1835 Ma) and prior to the onset of Yavapai subduction-related magmatism beginning around 1800 Ma. The pronounced subduction signature exhibited by trace elements in the dikes reflects derivation from mantle that was previously involved in Penokean subduction and arc accretion. The ca. 1813 Ma Hines quartz diorite that intrudes the Mountain shear zone in northeast Wisconsin (U-Pb zircon; Sims et al., 1990) and the 1813 ± 5 Ma Wissota dam tonalite (locality WD, Fig. 1, U-Pb zircon; Craddock et al., 2018) are the only other igneous ages reported in the 1835-1805 Ma interval (Sims et al., 1990).

The Biron dam mafic dikes strike east-northeast, normal to the overall Penokean convergence direction. Assuming they have not been significantly rotated since they were emplaced, their current orientation may suggest that these dikes represent a relaxation of Penokean northwest directed compression and a change to short-lived extensional tectonics, perhaps in the backarc region of a northwest-directed subducting slab. A similar interpretation of

back-arc extension preceding accretion has been proposed for the Penokean orogeny (Schneider et al. 2002; Schulz and Cannon, 2007). If so, this change to short-lived NW-SE extension may be the result of initiation of northwest subduction of Yavapai oceanic lithosphere beneath the accreted Marshfield terrane after Penokean orogenesis. Continued northwest-directed Yavapai subduction resulted in geon 17 magmatic activity into the Penokean province between 1805 and 1750 Ma prior to accretion of the Yavapai arc terrane during southward growth of the southern Laurentian margin (Holm et al., 2005; Van Schmus et al., 2007).

6.3 Age and extent of Proterozoic metamorphism and deformation in central Wisconsin

Our ca. 1817 Ma U-Pb zircon ages from the mafic dikes indicate that the amphibolite facies metamorphism and fabrics preserved at this locality in central Wisconsin must post-date Penokean orogenesis (Maass et al., 1980). Given the strong ductile deformation overprint exhibited in these rocks, it is critical to ascertain whether such overprinting was due to Yavapai, Mazatzal, or possibly even Wolf River associated tectonism (Schwartz et al., 2018). Published and new thermochronologic data presented here can help to correctly assign the age of tectono-metamorphic overprinting.

Our younger $^{40}\text{Ar}/^{39}\text{Ar}$ hornblende ages of ca. 1520-1530 Ma were obtained from samples collected at Conants Rapids, just 6-7 km from the western exposed edge of the 1470-1476 Ma Wolf River batholith, and our 1530 Ma $^{40}\text{Ar}/^{39}\text{Ar}$ muscovite age was obtained from a quarry within the EPSZ located 10-11 km from the Wolf River batholith. Holm et al. (2007) obtained three similarly young plateau or near-plateau $^{40}\text{Ar}/^{39}\text{Ar}$ hornblende ages (1514, 1438, and 1439 Ma) from country rock also collected near (<10-15 km) the Wolf River batholith. Together, these are the youngest hornblende cooling ages reported across the entire southern

Lake Superior region, and likely reflect the thermal effects of Wolf River magmatism upon the adjacent country rock, which has witnessed partial resetting of Ar systematics.

The 1672 Ma hornblende plateau age from metadiabase at Biron dam, located ~20 km from the Wolf River batholith, was likely not affected by Wolf River plutonism. Two independent lines of evidence support this interpretation. First, both theoretical time-governing equations on the thermal imprint of shallow level plutons (Carslaw and Jaeger, 1959) and direct field tests on large *shallow* intrusive bodies (i.e., the classic study by Hanson et al., 1975, on the extent of thermal effects of the Duluth gabbro on Archean country rock in northeastern Minnesota) indicate a spatially limited thermal aureole of ~10-12 km. Second, the 1600 Ma $^{40}\text{Ar}/^{39}\text{Ar}$ biotite plateau age (Holm et al., 2007) from the Biron dam locality falls within a tight cluster of <1620 Ma (1614-1576 Ma) mica $^{40}\text{Ar}/^{39}\text{Ar}$ plateau ages obtained over a large area of western Wisconsin – and up to distances of 170 km from the western edge of the exposed batholith. This uniformity of mica ages represents dominantly low-temperature (350-450 °C) Mazatzal-related resetting (Holm et al., 1998b; Romano et al., 2000), associated with widespread greenschist-facies metamorphism of most of the Wisconsin Magmatic terranes. Such low-grade geon 16 metamorphism is also pervasive in the 1750 Ma Montello batholith within the Yavapai terrane south of the WMT. Although granites and rhyolites in the Montello batholith preserve igneous structures on macro– and mesoscopic scales, they have been thoroughly recrystallized on the microscopic scale to albite-bearing greenschist facies mineral assemblages, and the Montello granite yields a whole-rock Rb–Sr isochron age of 1653 Ma (Van Schmus et al., 1975). The preservation of a 1600 Ma biotite $^{40}\text{Ar}/^{39}\text{Ar}$ plateau age at Biron dam is consistent with our interpretation that the Wolf River batholith did not thermally affect these rocks. Only bedrock mica $^{40}\text{Ar}/^{39}\text{Ar}$ ages that are younger than ca. 1600 Ma, such as geon 14–15 ages near the Wolf

River batholith and a few geon 11–12 ages north and west of the Wolf River batholith likely represent thermal resetting of previously Mazatzal reset micas. The 1672 Ma $^{40}\text{Ar}/^{39}\text{Ar}$ plateau age obtained here for Biron Dam hornblende, thus likely represents partial isotopic resetting of hornblende during Mazatzal greenschist-facies metamorphism.

We suggest that the 1817 Ma metadiabase dikes were initially deformed and metamorphosed under amphibolite facies conditions during the Yavapai orogeny, given that they intruded after Penokean orogenesis and experienced isotopic resetting during Mazatzal orogenesis. Holm et al. (2007) obtained a metamorphic monazite Pb–Pb age of 1744 ± 3 Ma from a coarse-grained garnet-staurolite schist in central Wisconsin (Hamburg Schist, locality HS, Fig. 1) and Van Wyck (1995) reported a preliminary 1722 Ma U–Pb titanite age on a metadiabase dike cutting a 1851 Ma granodiorite five km west of Biron dam. Additionally, Romano et al. (2000) obtained a 1733 ± 6 Ma hornblende $^{40}\text{Ar}/^{39}\text{Ar}$ plateau age in western Wisconsin. These data provide direct evidence for the existence of a late geon 17 middle amphibolite facies metamorphic episode in central Wisconsin. Our dike hornblende-plagioclase geothermometry data suggests Yavapai metamorphic temperatures reached as high as ~ 700 °C in this part of central Wisconsin. Strong folding with steeply plunging axes and a pervasive steep mineral lineation (Fig. 4c) can be attributed to the proximity of these rocks to the Spirit Lake tectonic zone, a Yavapai paleosuture (Fig. 1). A similar structural style of deformation marked by tight folds with steeply plunging axes in strata just north of the Niagara fault zone in northeast Wisconsin formed during earlier Penokean arc accretion (Larue, 1983).

6.4 Reheating and Stabilization of Proterozoic lithosphere

Conventional $^{40}\text{Ar}/^{39}\text{Ar}$ microcline plateau ages of ca. 1000 and 900 Ma (Fig. 7d) suggest the 1900-1700 Ma accreted Paleoproterozoic terranes finally cooled below 250 °C after 1100 Ma following extensive plume heating, volcanism, and associated widespread magmatic underplating during the MCR event. $^{40}\text{Ar}/^{39}\text{Ar}$ MDD feldspar thermochronology results yield more complex spectra signifying either slow cooling or resetting of MDD systematics during the MRS event. For instance, MDD results indicate the post-emplacement thermal history for the Wolf River batholith consisted of monotonic slow cooling of $\sim 0.5^\circ\text{C}/\text{Ma}$ throughout the late Proterozoic (Fig. 8b). Time-temperature histories suggest slow cooling continued to near-surface conditions of $\sim 45^\circ\text{C}$ by the early Cambrian, followed by Sauk transgression and Cambro-Ordovician heating of up to $\sim 150^\circ\text{C}$ or $\sim 3.17\text{-}4.75$ km of Paleozoic burial (assuming 20-30 °C/km geothermal gradients and 10 °C surface temperature; Fig. 8b). In contrast, feldspar sample PNG to the west of the Wolf River batholith (Fig. 1) likely experienced post-intrusion slow cooling through $\sim 300^\circ\text{C}$, followed by rapid cooling of $>4^\circ\text{C}/\text{Ma}$ at ca. 1100 Ma (Fig. 8b). Our southernmost sample (ILST-3) also shows rapid cooling ca. 1100 Ma, then slow cooling likely related to prolonged upper-crustal residence (1000-800 Ma) followed by more rapid cooling during the late Neoproterozoic.

Recent reconstructions of intermediate-temperature thermal histories of portions of the southern Canadian Shield suggest some amount of prolonged mid-crustal residence followed by significant (>5 km) exhumation at or after ca. 1.0 Ga caused by crustal thickening and isostatic uplift due to magmatic underplating (McDannell et al., 2018). Our inverse MDD modeling results provide additional thermal history information from Proterozoic provinces south of the Archean Superior Province, allowing for comparison of the effects of widespread MRS

magmatic underplating on Archean versus Proterozoic continental lithosphere. Although the currently exposed levels of both Archean and Proterozoic crust of the southern Canadian Shield display cooling at ca. 1.0 Ga, we interpret cooling of the Proterozoic province rocks to be related primarily to reheating of already shallow upper-crustal levels, not to exhumation of mid-crustal levels. The Baldwin conglomerate, which is intruded by the WRB, contains geon 14 detrital zircon grains indicating shallow conditions of batholith emplacement and limited exhumation of the region since geon 14 (Medaris et al., 2019). Shallow intrusion is consistent with rapid cooling of the batholith through ~ 300 °C, with limited metamorphic overprinting of the surrounding country rock (as described above for the Biron dam locality), and with the presence of miarolitic cavities in evolved plutons in the batholith (Anderson, 1980). Additionally, the presence of MRS dike swarms and evidence for localized resetting of $^{40}\text{Ar}/^{39}\text{Ar}$ isotopic systems further supports limited post-geon 14 exhumation of this region (Holm et al., 2007). The geologic evidence and country rock proximity to MRS rifting strongly favors early Neoproterozoic reheating of the shallow crust, rather than cooling via widespread exhumation as proposed for much of the Superior Province to the north (McDannell et al., 2018).

7. Conclusions

Our 1890 Ma zircon age for the Twelve Foot Falls quartz diorite sill near the Niagara suture zone demonstrates that the Pembine ophiolite formed at least 30 m.y. before its obduction during accretion of the Pembine-Wausau magmatic terrane. This minimum age is over 200 m.y. younger than rifting of Kenorland along the southern continental margin, indicating the likelihood of formation and closure of a major Paleoproterozoic ocean basin.

We identify a 30 m.y. gap in orogenic felsic magmatism following the Penokean orogeny during which only more mafic magmatism is documented (quartz diorite and diabase). We suggest that the 1835-1805 Ma interval in the southern Lake Superior region represents a fundamental period of tectonic switching (Collins, 2002) after the Penokean orogeny, when mafic magmatism was generated in an extensional back-arc setting during the initiation of north-directed Yavapai subduction. Subsequent 1805-1750 Ma metaluminous to peraluminous granitic magmatism could be related to a slab window or slab breakoff event during Yavapai subduction.

Until recently, metamorphic and deformational fabrics preserved in central Wisconsin have been attributed solely to Penokean orogenesis. However, our results indicate that the mafic dikes at Biron dam and Conants Rapids and their Penokean and Archean host rocks were strongly ductilely deformed at temperatures of ~ 700 °C during 1750-1720 Ma accretion of the Yavapai arc onto Penokean/Archean rocks along the Spirit Lake tectonic suture. Younger widespread medium temperature (300-400 °C) isotopic resetting occurred during Mazatzal regional metamorphic overprinting at 1650-1600 Ma. Geon 14 thermal overprinting was primarily restricted to a relatively narrow (10-15 km) contact zone surrounding the Wolf River batholith, consistent with its shallow depth of intrusion. Our results document that portions of the southern Penokean orogen preserve pervasive Yavapai structures, textures, and mineralogical compositions. Detailed, comprehensive investigations are needed to properly attribute variations in strain, structural style, and metamorphic overprinting to specific Proterozoic tectonomagmatic events in the northern US midcontinent region (Holm et al., 2007; Craddock et al., 2018).

At ca. 1.0 Ga, relatively young Proterozoic continental lithosphere of southern Laurentia was extensively underplated by mafic magmatism, which may have ultimately contributed to its

stabilization. In contrast, magmatic underplating of already stabilized Archean Superior Province lithosphere to the north caused it to be ‘destabilized’ and to undergo widespread exhumation.

Acknowledgments

This research was funded in part by National Science Foundation grant EAR-027432. We thank Bill Cannon and John Craddock for reviewing this manuscript.

Appendix A. Supplementary data

Supplementary Tables 1 and 2 associated with this article can be found online at <https://doi.org/10.1016/j.jprecamres.2019.105587>.

References

- Anderson, R., 1983. Proterozoic anorogenic granite plutonism of North America. *Geol. Soc. Am. Memoir* 161, 133-152.
- Armstrong, J.T., 1988. Quantitative analysis of silicates and oxide minerals: comparison of Monte-Carlo, ZAF and Phi-Rho-Z procedures: p. 239, in: *Proc. Microbeam Analysis Society*, ed. By D.E. Newbury, San Francisco Press, San Francisco.
- Carslaw, H.S., J.C. Jaeger, 1959. *Conduction of heat in solids*. 2nd ed. Oxford University Press, New York.
- Chichester, B., Rychert, C., Harmon, N., van der Lee, S., Frederiksen, A., Zhang, H., 2018. Seismic Imaging of the North American Midcontinent Rift Using S-to-P Receiver Functions: *Journal of Geophysical Res: Solid Earth*, 123. [Doi.org/10.1029/2018JB015771](https://doi.org/10.1029/2018JB015771).
- Collins, W.J., 2002. Hot orogens, tectonic switching, and creation of continental crust. *Geology* 30, 535-538.
- Compston, W., Williams, I.S., Meyer, C., 1984. U–Pb geochronology of zircons from lunar breccia 73217 using a sensitive high mass-resolution ion microprobe. *J. Geophysical Res.* (Suppl. 89), B525–B534.
- Craddock, J.P., Malone, D.H., Schmitz, M.D., Gifford, J., 2018. Strain Variations across the Proterozoic Penokean Orogen, USA and Canada: *Precambrian Res.* 318, 25-69.
- Dewane, T.J., Van Schmus, W.R., 2007. U-Pb geochronology of the Wolf River batholith, north-central Wisconsin: Evidence for successive magmatism between 1484 Ma and 1470 Ma. *Precambrian Res.* 157, 215-234.
- Dott, R.H., Jr., 1983. The Proterozoic red quartzite enigma in the north central United States: resolved by plate collision? *Geol. Soc. Am. Memoir* 160, 129-141.
- Gale, A., Dalton, C.A., Langmuir, C. II, Su, Y., Schilling, J.–G., 2013. The mean composition of ocean ridge basalts: *Geochemistry Geophysics Geosystems* 14, 489–518.
- Gallagher, K., 2012. Transdimensional inverse thermal history modeling for quantitative thermochronology. *J. Geophysical Res.: Solid Earth* 117(B2).
- Geiger, C., Guidotti, C., 1989. Precambrian metamorphism in the southern Lake Superior region and its bearing on crustal evolution. *Geosci. Wisc.* 13, 1-13.
- Halls, H.C., Davis, D.W., Stott, G.M., Ernst, R.E., Hamilton, M.A., 2008, The Paleoproterozoic Marathon large igneous province: New evidence for a 2.1 Ga long-lived mantle plume event along the southern margin of the North American Superior Province: *Precambrian Res.* 162, 327-353.

- Hanson, G.N., K.R. Simmons, A.E. Bence, 1975, Ar/Ar spectrum ages for biotite, hornblende and muscovite in a contact metamorphic zone: *Geochim. Cosmochim. Acta* 39, 1269-1277.
- Harrison, T.M., Lovera, O.M., Heizler, M.T., 1991. 40Ar/39Ar results for alkali feldspars containing diffusion domains with differing activation energy. *Geochim. Cosmochim. Acta* 55(5), 1435-1448.
- Harrison, T.M., Grove, M., Lovera, O.M., Zeitler, P.K., 2005. Continuous Thermal Histories from Inversion of Closure Profiles. *Rev. in Mineralogy and Geochemistry* 58(1), 389-409.
- Hinze, W.J., Allen, D.J., Braile, L.W., Mariano, J., 1997. The Midcontinent rift system: A major Proterozoic continental rift. *Geol. Soc. Am. Spec. Paper* 312, 7-35.
- Holland, T., Blundy, J. 1994. Non-ideal interactions in calcic amphiboles and their bearing on amphibole-plagioclase thermometry: *Contrib. Mineral. Petrol.* 116, 433-447.
- Holm, D.K, Lux, D., 1998. Depth of emplacement and tilting of the Middle Proterozoic (1470 Ma) Wolf River batholith, Wisconsin: Ar-Ar thermochronologic constraints. *Can. J. Earth Sci.* 35, 1143-1151.
- Holm, D., Darrach, K., Lux, D., 1998a. Evidence for widespread ~1760 Ma metamorphism and rapid crustal stabilization of the Early Proterozoic Penokean orogen, Minnesota. *Am. J. Sci.* 298, 60-81.
- Holm, D., Schneider, D.A., Coath, C., 1998b. Age and deformation of Early Proterozoic quartzites in the southern Lake Superior region: Implications for extent of foreland deformation during final assembly of Laurentia. *Geology* 26, 907-910.
- Holm D. K., Van Schmus, W. R., Mac Neil, L. C., Boerboom, T. J., Schweitzer, D., Schneider, D.A., 2005. U-Pb zircon geochronology of Paleoproterozoic plutons from the northern mid-continent, U.S.A.: Evidence for subduction flip and continued convergence after geon 18 Penokean orogenesis. *Geol. Soc. Am. Bull.* 117, 259-275.
- Holm, D.K., Schneider, D.A., Rose, S., Mancuso, C., McKenzie, M., Foland, K., Hodges, K.V., 2007. Proterozoic metamorphism and cooling ages from the southern Lake Superior region, USA: *Precambrian Res.* 157, 106-126.
- Hoppe, W., Montgomery, C., Van Schmus, W., 1983. Age and significance of Precambrian basement samples from northern Illinois and adjacent states: *Journal of Geophysical Research: Solid Earth* 88(B9), 7276-7286.
- Karlstrom, K.E., Bowring, S., 1993. Proterozoic orogenic history of Arizona, in Van Schmus, W. R., Bickford, M. E., 23 others, *Transcontinental Proterozoic provinces*, in Reed, J. C., Jr., and 6 others, eds., *Precambrian: Conterminous U.S.*: Boulder, Colorado, Geological Society of America, *The Geology of North America*, C-2, 188-211
- Karlstrom, K.E., Åhäll, K-I, Harlan, S.S., Williams, M.L., McLelland, J., Geissman, J.W., 2001. Long-lived (1.8–1.0 Ga) convergent orogen in southern Laurentia, its extensions to Australia and Baltica, and implications for refining Rodinia. *Precambrian Res.* 111, 5-30.

- Koppers, A.A.P. 2002. ArArCALC - software for $^{40}\text{Ar}/^{39}\text{Ar}$ age calculations. *Comp. & Geosci.* 28, 605-619.
- Larue, D.K., 1983. Early Proterozoic tectonics of the Lake Superior region; tectonostratigraphic terranes near the purported collision zone. *Geol. Soc. Am. Memoir* 160, 33-47.
- LaBerge, G.L., Cannon, W.F., Schulz, K.J., Klasner, J.S., Ojakangas, R.W., 2003. Paleoproterozoic stratigraphy and tectonics along the Niagara suture zone, Michigan and Wisconsin. In: Cannon, W.F. (Ed.), Part 2 – Field Trip Guidebook, Inst. Lake Superior Geol. 49, 1-32.
- Lovera, O.M., Richter, F.M., Harrison, T.M., 1989. The $^{40}\text{Ar}/^{39}\text{Ar}$ Thermochronometry for Slowly Cooled Samples Having a Distribution of Diffusion Domain Sizes. *J. Geophys. Res.* 94(B12), 17917-17935.
- Lovera, O.M., Heizler, M.T., Harrison, T.M., 1993. Argon diffusion domains in K-feldspar II: kinetic properties of MH-10. *Contrib. Min. Petrol.* 113, 381-393.
- Lovera, O.M., Grove, M., Mark Harrison, T., Mahon, K.I., 1997. Systematic analysis of K-feldspar $^{40}\text{Ar}/^{39}\text{Ar}$ step heating results: I. Significance of activation energy determinations. *Geochim. Cosmochimica Acta*, 61(15). 3171-3192.
- Lovera, O.M., Grove, M., Harrison, T.M., 2002. Systematic analysis of K-feldspar $^{40}\text{Ar}/^{39}\text{Ar}$ step heating results II: relevance of laboratory argon diffusion properties to nature. *Geochim. Cosmochimica Acta*, 66(7): 1237-1255.
- Ludwig, K.R., 2003. Isoplot/Ex, Version 3: A Geochronological Toolkit for Microsoft Excel. Geochronology Center Berkeley.
- Maass, R.S. 1983. Early Proterozoic tectonic style in central Wisconsin. In *Early Proterozoic geology of the Great Lakes region*. Edited by L.G. Medaris, Jr. *Geol. Soc. Am. Memoir* 160, 85-89.
- Maass, R.S., Medaris, L.G., Jr., Van Schmus, W.R., 1980. Penocean deformation in central Wisconsin. In: Morey, G.B., Hanson, G.N. (Eds.), *Selected studies of Archean gneisses and lower Proterozoic rocks, southern Canadian shield*. *Geol. Soc. Am. Memoir* 160, 85-95.
- McDannell, K.T., 2017. *Methods and application of deep-time thermochronology: Insights from slowly cooled terranes of Mongolia and the North American craton*. Theses and Dissertations. 2721, Lehigh University, Bethlehem, Pennsylvania, 261 p.
- McDannell, K.T., Zeitler, P.K., Schneider, D.A., 2018. Instability of the southern Canadian Shield during the late Proterozoic. *Earth and Planetary Science Letters*, 490: 100-109.
- McDougall, I., Harrison, T.M., 1999. *Geochronology and Thermochronology by the $^{40}\text{Ar}/^{39}\text{Ar}$ Method*, second ed. Oxford University Press, New York, p. 261.

- McDougall, I., Wellman, P., 2011. Calibration of GA1550 biotite standard for K/Ar and $^{40}\text{Ar}/^{39}\text{Ar}$ dating. *Chem. Geol.*, 280, 19-25.
- Medaris, G., Singer, B.S., Dott, R.H., Jr., Naymark, A., Johnson, C.M., Schott, R.C., 2003. Late Paleoproterozoic climate, tectonics and metamorphism in the southern Lake Superior region and Proto-North America: Evidence from Baraboo Interval quartzites. *J. Geology* 111, 243-257.
- Medaris, L.G. Jr., Schwartz, J.J., Singer, Bradley S., Jicha, B.R., 2018. Baraboo Interval quartzites: the Dott legacy and new revelations. *Geological Society of America, Programs with Abstracts*, 19-6.
- Medaris, L.G. Jr., Malone, D.H., Hill, G.C., Singer, Bradley S., Jicha, B.R., Van Lankvelt, A., Williams, M.L., Reiners, P.W., 2019. The Wolf River Orogeny: Geon 14 Magmatism, Sedimentation, and Deformation in the Southern Lake Superior Region: *Institute on Lake Superior Abstracts*, 65, 45-46.
- Murphy, J. Brendan, 2007. Igneous rock associations 8. Arc magmatism II: geochemical and isotopic characteristics: *Geoscience Canada*, 34, 7–35.
- Myers, P.E., Cummings, M.L., Wurdinger, S.R., 1980. Precambrian geology of the Chippewa valley, Wisconsin. 26th Ann. Inst. Lake Superior Geol., Guidebook, Field Trip 1, 35-123.
- NICE Working Group, 2007. Reinterpretation of Paleoproterozoic accretionary boundaries of the north-central United States based on a new aeromagnetic-geologic compilation. *Precambrian Res.* 157, 71-79.
- Ola, O., Frederiksen, A., Bollmann, T., van der Lee, S., Darbyshire, F., Wolin, E., Revenaugh, J., Stein, C., Stein, S., Wysession, M., 2016. Anisotropic zonation in the lithosphere of Central North America: influence of a strong cratonic lithosphere on the Mid-Continent Rift. *Tectonophysics* 683, 367-381.
- Paces, J.B., Miller, J.D., 1993. Precise U–Pb age of Duluth Complex and related mafic intrusions, northeastern Minnesota: geochronological insights into physical, petrogenetic, paleomagnetic, and tectonomagmatic processes associated with the 1.1 Ga midcontinent rift system. *J. Geophysical Research* 98, 13997–14013.
- Parrish, R. R. 1990. U-Pb dating of monazite and its application to geological problems, *Can. J. Earth Sci.* 27(11), 1431–1450.
- Pietrzak-Renaud, N., and Davis, D., 2014. U-Pb geochronology of baddeleyite from the Belleview metadiabase: Age and geotectonic implications for the Negaunee Iron Formation, Michigan, *Precambrian Res.* 250, 1-5.
- Price, W.L., 1977. A controlled random search procedure for global optimisation. *The Computer Journal*, 20(4): 367-370.

- Reiners, P.W., Ehlers, T.A., Zeitler, P.K., 2005. Past, present, and future of thermochronology. In: P.W. Reiners and T.A. Ehlers (Editors), *Low-Temperature Thermochronology: Techniques, Interpretations, and Applications*. Reviews in Mineralogy and Geochemistry. Mineralogical Society of America and Geochemical Society, Washington, DC, United States, pp. 1-18.
- Renne, P., Swisher, C. Deino, A., Karner, D., Owens, T., DePaolo, D., 1998. Intercalibration of standards, absolute ages and uncertainties in $^{40}\text{Ar}/^{39}\text{Ar}$ dating. *Chem. Geol.* 145, 117-152.
- Romano, D., Holm, D.K., Foland, K., 2000. Determining the extent and nature of Mazatzal-related overprinting of the Penokean orogenic belt in the southern Lake Superior region, north-central USA. *Precambrian Res.* 104, 25-46.
- Schmitt, A., Grove, M., Harrison, T.M., Lovera, O.M., Hulen, J., Waters, M., 2003. The Geysers–Cobb Mountain Magma System, California (Part 1): U–Pb zircon ages of volcanic rocks, conditions of zircon crystallization and magma residence times. *Geochim. Cosmochimica Acta* 67, 3423–3442. doi:10.1016/S0016-7037(03) 00140-6.
- Schneider, D.A., Bickford, M.E., Cannon, W., Shulz, K., Hamilton, M., 2002. Age of volcanic rocks and syndepositional iron formations, Marquette Range Supergroup: implications for the tectonic setting of Paleoproterozoic iron formations of the Lake Superior region. *Can. J. Earth Sci.* 39, 999-1012.
- Schneider, D.A., Holm, D.K., O’Boyle, C., Hamilton, M., Jercinovic, M., 2004. Paleoproterozoic development of a gneiss dome corridor in the southern Lake Superior region, USA: *In* Whitney et al. (eds) *Gneiss domes in orogeny*: *Geol. Soc. Am. Special Paper* 380, 339-357.
- Schulz, K.J., 1987. An Early Proterozoic ophiolite in the Penokean orogen [Abstract]: Geological Society of Canada—Mineralogical Association of Canada, Program with Abstracts, v. 12, p. 87.
- Schulz, K.J., Cannon, W.F., 2007. The Penokean orogeny in the Lake Superior region. *Precambrian Res.* 157, 4-25.
- Schulz, K.J., Cannon, W.F., Woodruff, L.G., 2018. Geochemistry of mafic rocks in Dickinson County, Michigan: Evidence for ~2.1 Ga Rifting, 64th Institute on Lake Superior Geology Proceedings, v. 64, Part 1, Program and Abstracts, p. 93-94
- Schumacher, J.C, 1997. The Estimation of the proportion of ferric iron in the electron-microprobe analysis of amphiboles, Appendix 2 in Leake B.E. and 21 others, *Nomenclature of amphiboles: Report of the subcommittee on amphiboles of the International Mineralogical Association, Commission on new minerals and mineral names: Canadian Mineralogist* 35, 219-249.
- Schwartz, Joshua J., Stewart, Esther K., Medaris, L. Gordon Jr., 2018. Detrital Zircons in the Waterloo Quartzite, Wisconsin: Implications for the Ages of Deposition and Folding of Supermature Quartzites in the Southern Lake Superior Region, 64th Institute on Lake Superior Geology Proceedings, v. 64, Part 1, 95-96.

- Sims, P. K., 1993. Petrography and geochemistry of early Proterozoic granitoid rocks in Wisconsin Magmatic terranes of Penokean Orogen, northern Wisconsin, US Government Printing Office, v. 1904.
- Sims, P.K, Van Schmus, R., Schulz, K., Peterman, Z., 1989. Tectono-stratigraphic evolution of the Early Proterozoic Wisconsin magmatic terranes of the Penokean orogen. *Can. J. Earth Sci.* 26, 2145-2158.
- Sims, P.K., Klasner, J.S., Peterman, Z.E., 1990. The Mountain shear zone, northeastern Wisconsin, U.S.A. – a ductile deformation zone within the Early Proterozoic Penokean orogeny. *USGS Bulletin* 1904-A.
- Sims, P.K., Schulz, K.J., Peterman, Z.E., 1992. Geology and geochemistry of Early Proterozoic rocks in the Dunbar area, northeastern Wisconsin: U.S. Geological Survey Professional Paper 1517, 65 p.
- Sims, P.K., Schulz, K.J., 1993, Geologic map of Precambrian rocks in parts of Iron Mountain and Escanaba 30' X 60' quadrangles, northeastern Wisconsin and adjacent Michigan: U.S. Geological Survey Miscellaneous Investigations Series Map 1-2356, scale 1:100,000
- Smith, M.E., Singer, B.S., Carroll, A.R., Fournelle, J.H. (2006) High-resolution calibration of Eocene strata: $^{40}\text{Ar}/^{39}\text{Ar}$ geochronology of biotite in the Green River Formation. *Geology* 34, 393-396.
- Stewart, E.D., Stewart, E.K., Walker, Alex, Zambito, J, J., Jr., 2018. Revisiting the Paleoproterozoic Baraboo interval in southern Wisconsin: evidence for syn-depositional tectonism along the south-central margin of Laurentia: *Precambrian Res.*, 314, 221–239.
- Van Schmus, W.R., Hinze, W.J., 1985. The Mid-Continent Rift System, *Annual Rev. Earth Planet. Sci.* 13, 345-383.
- Van Schmus, W.R., Thurman, M.E., Peterman, Z.E., 1975. Geology and Rb-Sr chronology of Middle Precambrian rocks in eastern and central Wisconsin. *Geol Soc. Am Bull.* 86, 1255-1265.
- Van Schmus, W.R., 1980. Chronology of igneous rocks associated with the Penokean orogeny in WI. *In* Morey and Hanson (eds) *Selected studies of Archean gneisses and lower Proterozoic rocks, southern Canadian Shield.* *Geol. Soc. Am. Spec. Paper* 182, 159-168.
- Van Schmus, W.R., Schneider, D.A., Holm, D.K., Dodson, S., Nelson, B.K., 2007. New insights into the southern margin of the Archean-Proterozoic transition in the north-central U.S. based on U-Pb, Sm-Nd, and Ar-Ar geochronology. *Precambrian Res.* 157, 80-105.
- Van Wyck, N., 1995. Oxygen and carbon isotopic constraints on the development of eclogites, Holsnøy, Norway, and major and trace element, common lead, Sm-Nd, and zircon geochronology constraints on petrogenesis and tectonic setting of pre- and Early Proterozoic rocks in Wisconsin. Unpublished Ph.D. thesis, University of Wisconsin, 288 pp.

Willett, S.D., 1997. Inverse modeling of annealing of fission tracks in apatite 1: A controlled random search method. *Am. J. Science*, 297(10): 939-969.

Williams, H., Hoffman, P.F., Lewry, J.F., Monger, J.W.H. Rivers, T. 1991. Anatomy of North America: thematic geologic portrayals of the continent. *Tectonophysics* 187, 117-134.

Zeitler, P.K., 2004, Arvert 4.1. Inversion of $^{40}\text{Ar}/^{39}\text{Ar}$ Age Spectra., User's Manual 2004, updated Nov. 2017 <http://eesarchive.lehigh.edu/EESdocs/geochron/software.html>.